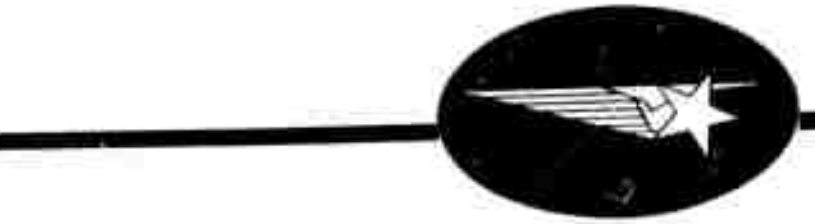

QSTS 3rd - Limited

HIGH-EFFICIENCY, SINGLE-FREQUENCY LASER AND MODULATOR STUDY

5th Quarterly Summary Technical Status Report

N-JY-71-10 31 December 1971

R. C. Ohlmann, W. Culshaw, K. K. Chow, H. V. Hance, W. B. Leonard, and J. Kannelaud

Contract No. N00014-71-C-0049
ARPA Order No. 306
Program Code 421
Effective Date of Contract: 1 September 1970
Expiration Date: 31 October 1972
Amount: $284,900
Scientific Officer: Director, Physics Programs
Physical Sciences Division
Office of Naval Research, Arlington, Va. 22217
Principal Investigator: R. C. Ohlmann (415) 493-4411, ext. 45275

Sponsored by the
Advanced Research Projects Agency
ARPA Order No. 306

Lockheed Palo Alto Research Laboratory
LOCKHEED MISSILES & SPACE COMPANY, INC.
A Subsidiary of Lockheed Aircraft Corporation
Palo Alto, California 94304

CONTENTS

ILLUSTRATIONS

Section 1
INTRODUCTION

The general objective of this research and development program is to conduct investigations that will contribute to the development of an ultrawide-bandwidth laser communication system. The specific objectives are: (1) a study of laser communication system configurations, particularly modulation formats, that are most suitable for very high data rates up to 2 Gbit/sec; (2) research on high-efficiency, single-frequency Nd:YAG lasers as the transmitter source for such a communication system; and (3) research on an optical modulator with 2 GHz of rf bandwidth and good modulation efficiency.

The primary emphasis of the program is on objectives (2) and (3). However, a considerable body of work on the first objective, the study of optical communication modulation formats, is being completed and will be presented in the next quarterly report. In addition, work has continued on improving the efficiency of the Nd:YAG single-frequency laser and on the extension of the bandwidth of the optical modulator.

1.1 LASER COMMUNICATION SYSTEM CONFIGURATIONS

A number of modulation formats that have potential value for high-data-rate laser communications have been evaluated. The modulation formats studied include baseband and subcarrier techniques suitable for cw or pulse-laser outputs. The baseband formats considered are the M-ary and binary on-off modulation and binary polarization modulation. The subcarrier formats are those in which the information is impressed on an rf subcarrier before it modulates the laser beam. Applicable subcarrier formats are digital phase modulation of the subcarrier, both biphase and quadriphase, and amplitude and frequency modulation.

The modulation formats have been compared on the basis of their communication efficiency, specifically the number of photons per bit required at the receiver to achieve a given

bit error rate. The comparison shows that the choice of format depends heavily on the bit rate because of component limitations at high bit rates. Thus, the M-ary on-off modulation is most efficient up to bit rates of about 100 Mbits/sec, but above that rate electronic and modulator implementation is not easily achievable. Binary polarization modulation is next most efficient up to a few hundred megabits per second, but becomes less efficient at higher rates because of system losses and modulation efficiency. Quadriphase shift keying of a subcarrier is almost as efficient as binary polarization modulation and has the advantage that rates up to 2 Gbit/sec can be implemented. These results are being finalized for inclusion in the sixth quarterly report.

1.2 EFFICIENT SINGLE-FREQUENCY Nd:YAG LASERS

Previously we reported that 0.8W of single-frequency output power has been attained from a Nd:YAG laser pumped with a 1-kW tungsten lamp. This was done using a single mode filter consisting of a tilted Fabry-Perot etalon and a metal-film etalon in the cavity, along with a technique for achieving a large TEM_{00} waist diameter in the laser rod. However, the stability of this output was a sensitive function of the transverse alignment of the mode within the laser rod, and of the thermal fluctuations in the rod.

In this reporting period we have concentrated on improving the laser structure design to increase stability, and have investigated techniques for significantly increasing efficiency. The efficiency increase is being sought primarily by proper use of potassium-rubidium (K-Rb) lamps to pump the laser, along with better mode design and lower intracavity losses.

The visible and IR spectra and the intensity distribution across the K-Rb lamp diameter has been obtained as a necessary prelude to effective employment of these lamps. A further increase in stability can be achieved with a larger waist diameter in the laser rod. However, the heating of the rod and the water jacket around it causes instabilities at large waist diameters. Thus, we have investigated means of filtering the infrared radiation from the lamp without decreasing the pumping efficiency of the radiation in the pump bands.

1.3 WIDE-BANDWIDTH ELECTROOPTICAL MODULATOR

Earlier in this program we reported on an electrooptical modulator which efficiently modulated a laser beam throughout the frequency band of 1 to 2 GHz. The study has been extended to cover research, design, and test of a modulator in the 2- to 4-GHz band so as to achieve 2 GHz of rf bandwidth capable of carrying 2 Gbit/sec of data.

During this quarter, a 50-Ω impedance, 2- to 4-GHz band modulator has been designed and fabricated, using the principles previously established on this program. RF tests indicate that the modulator will accommodate a $LiNbO_3$ crystal of 7-mm length giving essentially the design bandwidth. To evaluate modulators in this frequency range, techniques for measuring modulation depth have been developed: Three methods of calibrating photodetectors in the 2- to 4-GHz band have been found useful. Studies of crystal fabrication techniques were also pursued since it was found difficult to maintain optical quality while fabricating crystals of typical dimensions 0.3 by 0.3 by 7 mm. However, polarization extinction ratios as high as 25 dB have been now obtained on selected 5-mm- and 9-mm-long $LiNbO_3$ crystals.

Section 2
EFFICIENT Nd:YAG LASER DESIGN

The purpose of the laser research and development part of this program is to design and develop a highly efficient cw, TEM_{oo}-mode, single-frequency Nd:YAG laser having 1-W output at 1.06 μm. Experimental evidence obtained on previous programs reviewed below indicates that pumping the laser with a potassium-rubidium (K-Rb) vapor lamp is the technique most likely to achieve success in meeting the efficiency goal. However, many problems must be solved to employ this design in a laser having suitable characteristics. The following sections review these problems and the solutions which are being studied.

The solution to these problems involves the development of techniques that may be broadly subdivided into three categories:

(1) The technique of obtaining maximum TEM_{oo}-mode efficiency using a Nd:YAG laser rod pumped by an optimum K-Rb lamp, with particular reference to the laser physics of Nd:YAG lasers. This problem area involves the spectroscopy of Nd:YAG and the lamps, as well as the TEM_{oo}-mode volume, the saturation parameters, and the threshold conditions.

(2) The technique of maximum coupling of the lamp radiation to the laser rod while maintaining the lamp at its optimum operating point. This problem area involves the lamp characteristics while operating in the pumping cavity, the pumping cavity design for maximum coupling, and the techniques for filtering the lamp radiation.

(3) The technique of obtaining stable single-frequency operation at 1.06 μm with minimum insertion loss of the mode filter.

The efforts on these categories during the last quarter have concentrated primarily on developing a design based on deep understanding of the lamp, the pumping cavity, and the single-frequency mode filter problem. Experiments were performed to better

characterize the lamp spectrum and its effective radiating dimensions. Studies of the pumping cavity were aimed at a better determination of the focusing properties of spherical enclosures. In addition, means to use this cavity to absorb the excess infrared radiation from the lamp rather than in the laser rod or water filter around the rod were considered. This effort is aimed at increasing the stability of the single-frequency laser by decreasing thermal fluctuations in the laser rod.

2.1 LASER PHYSICS OF EFFICIENT CW TEM_{oo}-MODE Nd:YAG LASERS

The efficiency of a Nd:YAG laser operating in the TEM_{oo}-mode depends on a large number of parameters. Theoretical analysis can provide a guide to parameter optimization to maximize efficiency, but the final design must be developed emprically, based on experimental results. A brief theoretical review of the relevant physics, including some experimental observations on the spectra of K-Rb lamps and of Nd:YAG, is presented below.

2.1.1 Spectroscopy of Nd:YAG and K-Rb Lamps

It is well known that Nd:YAG can operate as an "approximately" four-level laser system when optically pumped in its absorption bands at wavelengths shorter than 0.9 μm. About 10^{-5} of the Nd^{3+} population is in the terminal state of the laser transition near room temperature, so that the excess gain of the material when pumped as a laser starts at about -0.1%/cm rather than at zero, as it would for a true four-level laser.

The terminal level of the laser transition in the $^4I_{11/2}$ manifold is 2109 cm^{-1} above the ground state of the $^4I_{9/2}$ manifold (Ref. 2-1). The originating level of the laser transition at 1.0641 μm is the upper state of the $^4F_{3/2}$ double at 11510 cm^{-1}. The principal useful absorption of pump light from K-Rb lamps is in the bands between 7300 and 8300 A, with some absorption out to 9000 A. Energy absorbed in these bands rapidly thermalizes to the $^4F_{3/2}$ manifold.

There is also some absorption by Nd^{3+} on the near-infrared by transitions into the $^4I_{15/2}$ manifold at about 6000 cm^{-1} (1.48 – 1.78 μm), the $^4I_{13/2}$ manifold at about

4000 cm^{-1} (2.21 – 2.7 μm), and the $^4I_{11/2}$ manifold at 2200 cm^{-1} (4 – 5 μm). YAG itself begins to absorb at about 4.5 μm, and a 2-mm-thick slab is completely absorbing at 6.2 μm. The quantitative absorption and transmission spectra of Nd:YAG taken at LMSC are given in Figs. 2-1 and 2-2. The emission spectrum of an optimum pressure K-Rb lamp is reproduced in Fig. 2-3 (Ref. 2-2), and an infrared spectrum of the lamp is presented in Fig. 2-4.

In addition to the well-known conclusion that K-Rb lamps are effective in exciting Nd:YAG in the 0.7- to 0.9-μm pump bands (Ref. 2-3), two observations concerning the infrared bands are significant for the present program. Absorption into the ^4I bands can have the effect of increasing the laser terminal state population, thus increasing the threshold for laser oscillation. However, it requires extremely high pumping rates for this to occur, since the radiationless transitions that thermalize the terminal level population are very fast (estimated as $\approx 10^{-7}$ to 10^{-11} sec). A continuously pumped Nd:YAG with 1-W output is unlikely to be excited sufficiently rapidly to cause any excess population buildup in the terminal level.*

Using the present technique of cooling the Nd:YAG rod with a 2.75-mm-thick layer of flowing water, most of the infrared radiation from the lamp beyond 1.4 μm is absorbed, as can be seen from the transission curve for water shown in Fig. 2-5. Comparing the lamp spectrum (Fig. 2-4), the Nd:YAG absorption spectrum (Fig. 2-1) and the water filter transmission, it can be seen that there will be negligible pumping of Nd:YAG in the ^4I bands. The Nd:YAG is not absorbing at the wavelength of the two strong K-Rb lamp lines at 1.13 and 1.23 μm that can pass through the water filter.

The major problem with absorbing several hundred watts of power in the water filter is the resulting noise produced in the laser output. This noise comes from two sources; first, the flow rate must be about 2 gal/min in order to keep the rise in water temperature down to a few degrees as rise water passes over the length of the rod, and this

*To take an extreme example, if 10 W were directly absorbed in the terminal level which decayed with a 10^{-7}-sec time constant, the excess population buildup would be only 2% of the thermal population at 0°C.

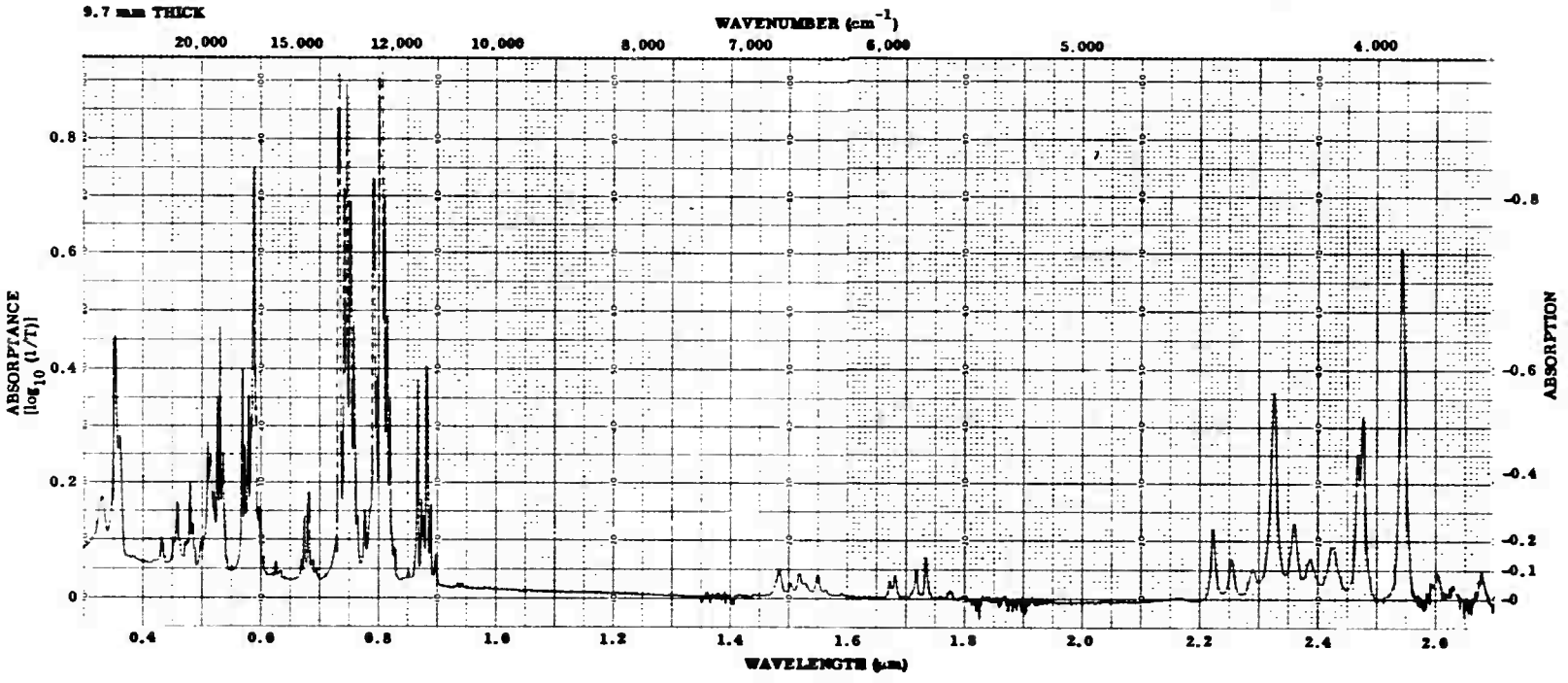

Fig. 2-1 Absorptance Spectrum [$\log_{10}$ (1/transmission)] of a 9.7-mm-Thick Sample of Nd:YAG ($\approx$1.0 at. % Nd) From 0.3 to 2.7 μm

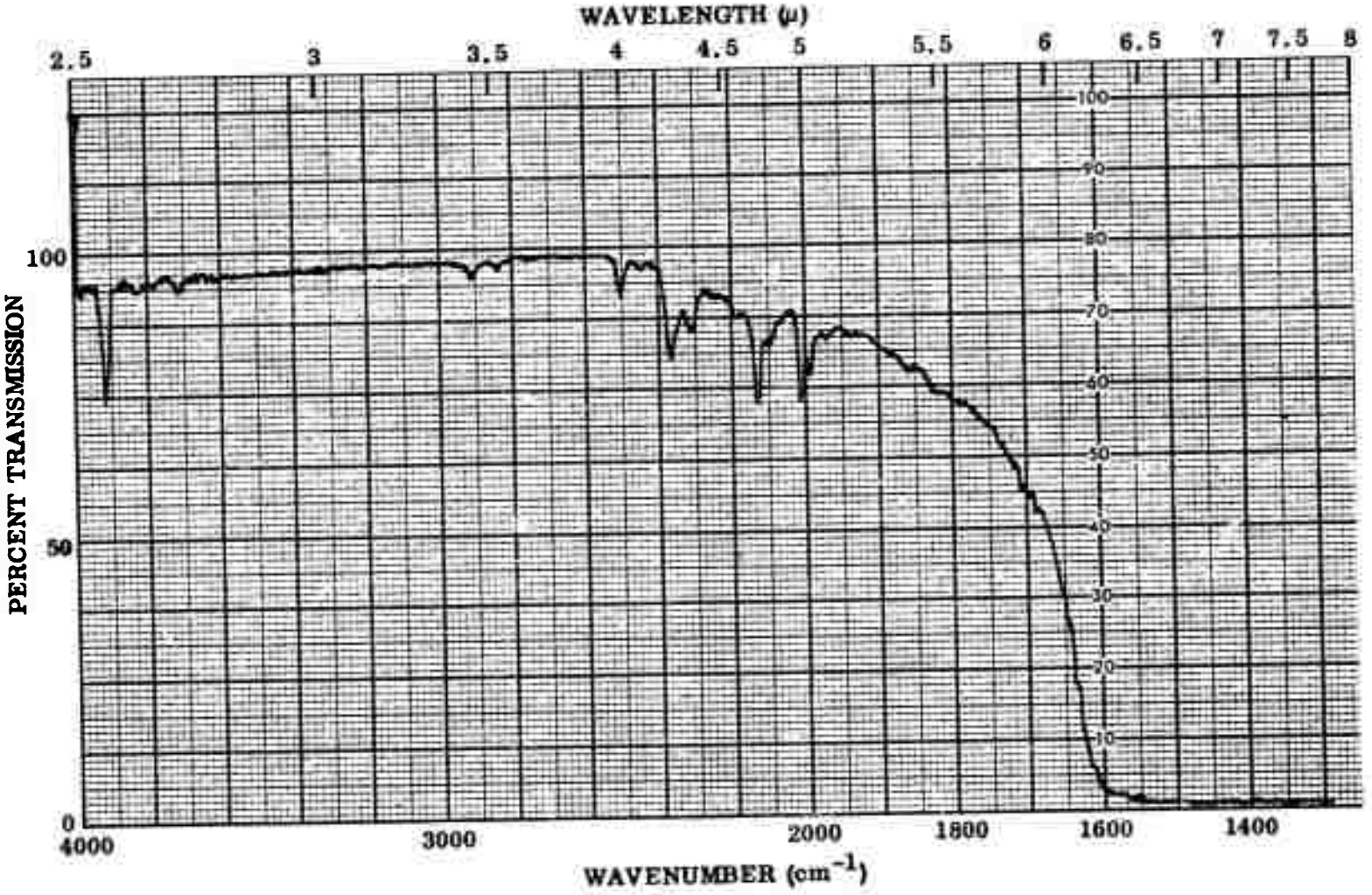

Fig. 2-2 Transmission Spectrum of a 1.9-mm-Thick Sample of Nd:YAG (≈ 1.0 at. % Nd) From 2.5 to 8.0 μm

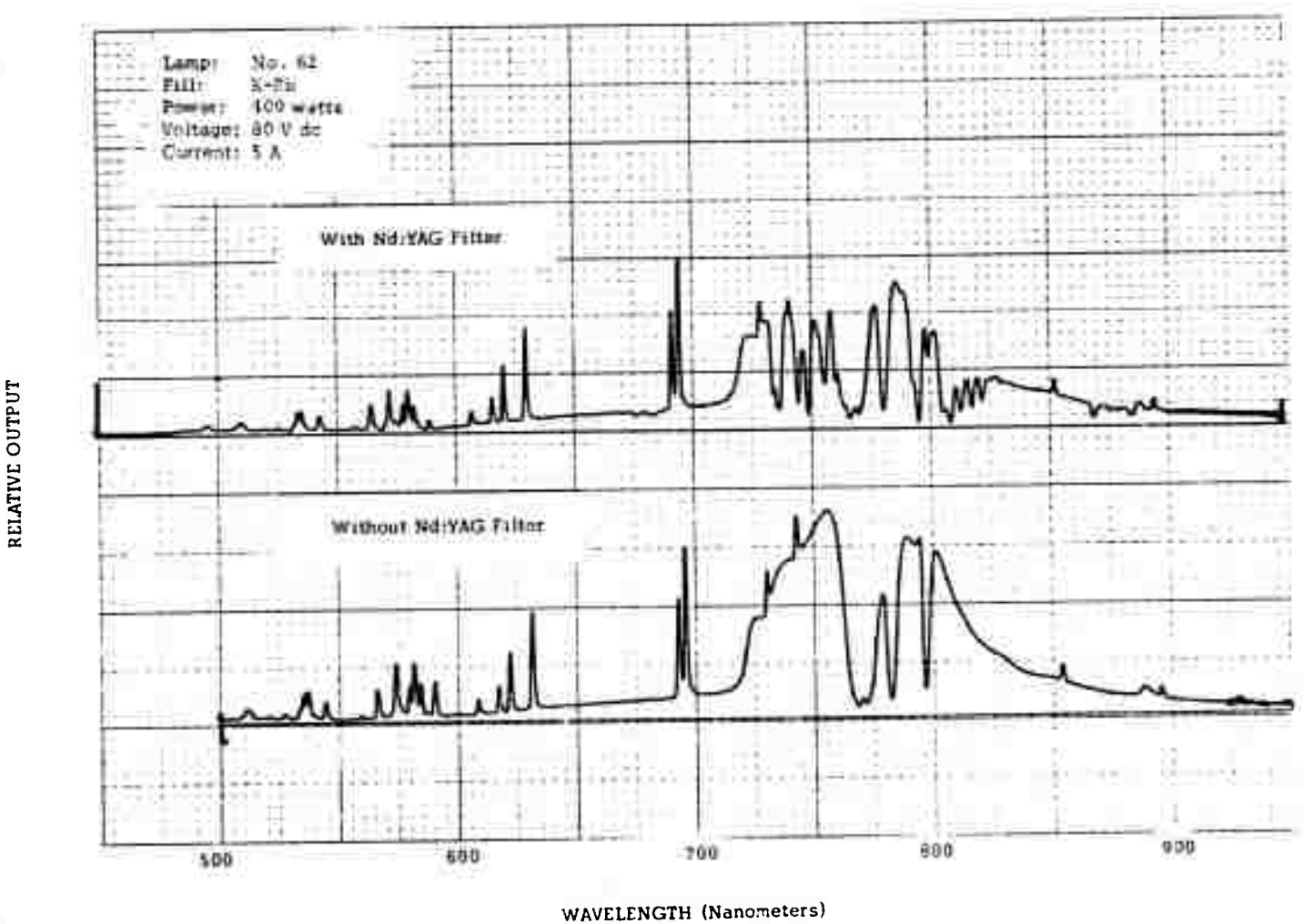

Fig. 2-3 Emission Spectra and Nonabsorbed Radiation of Optimum Pressure Rubidium Potassium Lamp (Ref. 2-2)

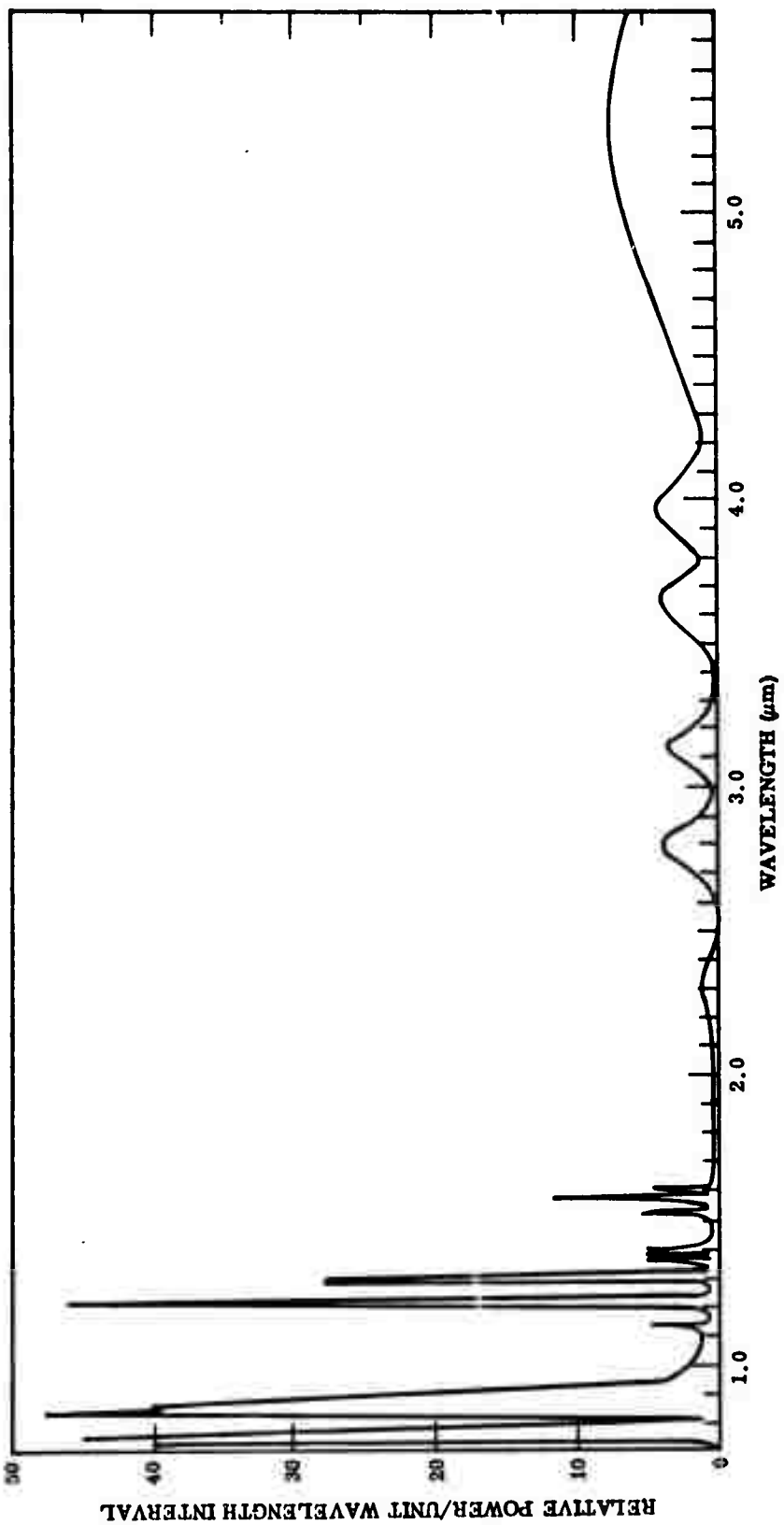

Fig. 2-4 Emission Spectrum From 0.6 to 5.7 μm of a K-Rb Vapor Lamp Operated Under Conditions for Optimally Exciting Nd:YAG. Ordinate is in relative power per unit wavelength interval.

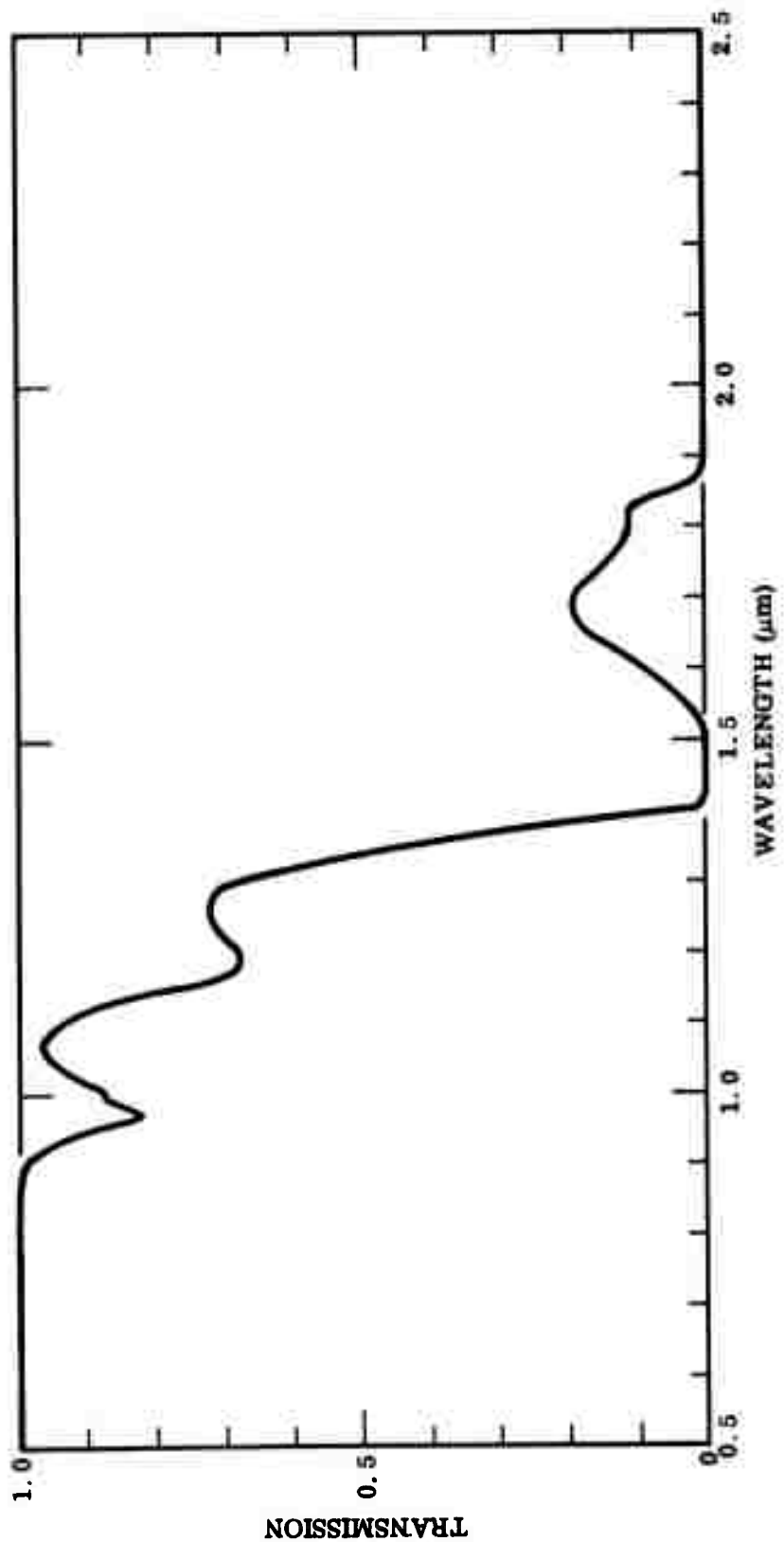

Fig. 2-5 Transmittance of 3 mm of Water, Corrected for Reflection

causes some vibrational noise in the laser rod; second, the incomplete turbulence of the water causes some temperature fluctuations on the surface of the rod which vary its internal optical path and birefringence. Therefore, a design is being developed to reduce the heat input to the water layer so the flow rate can be reduced.

One way of reducing the heat input is to place a second water filter around the lamp. This filter must consist of two concentric tubes since water cannot flow directly on the lamp surface. However, the extra losses due to reflections from four surfaces of the tubes result in a decrease of pumping efficiency by 15 to 20%. A better way to perform this absorption of the unwanted infrared radiation is in the sphere itself. This technique is being studied in the present quarter.

2.1.2 Output Power of a CW Nd:YAG Laser

The steady-state output power of a laser, P_{out}, can be written in terms of the laser gain, the losses, and the saturation parameter as follows (Ref. 2-4):

$$P_{out} = \frac{T}{2S}\left[\frac{2\,g_o - (L + T)}{L + T}\right] \qquad (2.1)$$

where

g_o = unsaturated single-pass excess gain over unity

S = saturation parameter of the laser

L = double-pass cavity loss

T = transmission of the output mirror (the other laser mirror losses are included in L)

By selecting the optimum transmission of the output mirror,

$$T_{opt} = (2\,g_o\,L)^{1/2} - L \qquad (2.2)$$

the output power is then a maximum and is equal to

$$P_{out}^{max} = (2S)^{-1} \left(\sqrt{2\, g_o} - L\right)^2 \tag{2.3}$$

The expected output power is determined from Eq. (2.3) after inserting experimental v values for the three parameters.

Saturation Parameter. The saturation parameter can be written for TEM_{oo}, multi-longitudinal-mode operation as

$$(2S)^{-1} \cong \pi\, \omega_L^2\, h\nu/\sigma\tau \tag{2.4}$$

where

ω_L = mode waist radius in laser rod
$h\nu$ = energy per laser photon
σ = peak laser transition cross section
τ = fluorescence decay time

Equation (2.4) is approximate because it involves a linearization of the exact expressions derived by Poloni and Svelto (Ref. 2-5). The theoretical value of $(2S)^{-1}$ for Nd:YAG at 0°C is determined by substituting $\sigma \approx 10^{-18}$ cm^2, $\tau \approx 2.5 \times 10^{-4}$ sec, and $h\nu = 1.87 \times 10^{-19}$ J (Ref. 2-6), so that $(2S)^{-1} = (\pi\, \omega_L^2) \times 750$ (W/cm^2).

It is obvious that the waist should be as large as practical for maximum output power if the gain does not decrease with large waist. We have been able to use a TEM_{oo}-mode waist radius of $\omega_L = 0.12$ cm in a 6-mm-diameter Nd:YAG rod, which resulted in $(2S)^{-1} \simeq 40$ W. One published report uses a waist of ≈ 0.1 cm, so a value of $(2S^{-1}) = 25$ W was achieved (Ref. 2-4). The practical limit to the waist size is set by the tradeoff between laser stability, maximum gain for a given lamp diameter, and losses. For single-frequency operation with spatial saturation in the rod, the effective saturation parameter is reduced to about 50% of the above values.

Gain. It is useful to express g_o in terms of cavity pumping parameters. The gain may be written as

$$g_o = K (P_{lamp} - P_o) \tag{2.5}$$

where

- K = constant proportional to lamp conversion efficiency, efficiency of focusing, efficiency of absorption per unit volume, and the laser material parameters
- P_{lamp} = electrical power into the lamp
- P_o = lamp power required to overcome terminal level population and to warm up the lamp

In a recent report it was estimated that the product of K times the rod diameter d is approximately constant (Ref. 2-7). This was based on only one experimental data point. Theoretically, it would be true only if the lamp image were much smaller than the rod and the rod were relatively strongly absorbing so that the incident radiation were heavily attenuated before it reached the center of the rod. Neither of these conditions is true for pumping Nd:YAG rods. Data on the effective lamp diameter are given below. The gain expected for a 3-mm-diameter rod should be only slightly higher than for a 5-mm-diameter rod.

In order to predict the output power using a K-Rb lamp, the gain expected using 300-W input power must be estimated. Liberman (Ref. 2-8) has measured a Nd:YAG laser output using a 1-in.-long K-Hg lamp and has found that an input power of 300 W to the K-Hg lamp was equivalent in pumping Nd:YAG to using a tungsten lamp at 800-W input. These data (on a lamp too heavily loaded) indicate that a gain of almost 5% is feasible with the K-Hg lamp at 300-W input. However, Noble (Ref. 2-2) finds that a 2.5-in.-long lamp at 300 W is equivalent to a 450-W Kr lamp in pumping Nd:YAG, which means that a gain of greater than 3% would be attainable using that K-Rb lamp at 300-W input if Kr lamps have somewhat higher efficiencies than tungsten lamps.

Losses. It should also be noted from Eq. (2.3) that losses must be kept low to achieve the required output. These losses arise from the scattering at the end mirrors, the reflection off the laser rod faces, the losses internal to the rod, and the aperture loss to maintain TEM_{oo} -mode operation and reject higher order modes. Due to the multilayer coatings used for the mirrors, they typically have scattering losses of 0.2% each, or 0.4% total "round trip." The standard antireflection (AR) coatings are quoted as having 0.1% reflectivity, yielding a 0.4% loss round-trip for two surfaces. Aperturing for sufficient off-axis mode rejection may require 0.15% TEM_{oo}-mode loss in each direction, for a total round-trip loss of 0.3%. Adding 0.2% material loss, a total round-trip loss of 1.3% minimum is expected.

The loss due to the thermal distortion of the laser rod is estimated as 0.2%. Lamp filtering techniques will minimize the heat input to the rod, so only a few watts of heat will be generated in the rod. The degree of distortion and loss produced by this heat when the rod is conductively cooled is subject to further experimental investigation.

TEM_{oo}-Mode Power Output. A plot of Eq. (2.3), the expected output power as a function of g_o for several values of L, is given in Fig. 2-6. It is seen that in order to reach 1-W output power in the TEM_{oo}-mode with an estimated double-pass loss of 1.3%, the single-pass gain must be 3.7% if the saturation parameter is $(2S)^{-1}$ = 40 W. Note that this saturation parameter requires a waist radius of about 1.2 mm in the rod. The curve of Fig. 2-6 has some experimental confirmation, since we have achieved almost 3 W of TEM_{oo} power output using a waist of 1.1 mm. A 6-mm-diameter by 30-mm-long rod was pumped in a sphere by a 1000-W tungsten lamp. The single-pass gain was estimated at about 6%. This output is somewhat higher than predicted by theory, indicating that the saturation parameter or gain was underestimated. Another confirmation is given by the results of Geusic (Ref. 2-4), where a 1.3-W output is calculated using Eq. (2.3) and 1.1 W was achieved.

On the basis of Fig. 2-6 and the experimental data, we expect to achieve at least 1-W TEM_{oo}-mode laser output using 300-W input to a K-Rb vapor lamp. If a single-pass gain of 5% can be obtained and losses can be kept to 1.5% (round trip), a single-frequency output of 1 W should be obtained even with a lower saturation parameter (1/2 S).

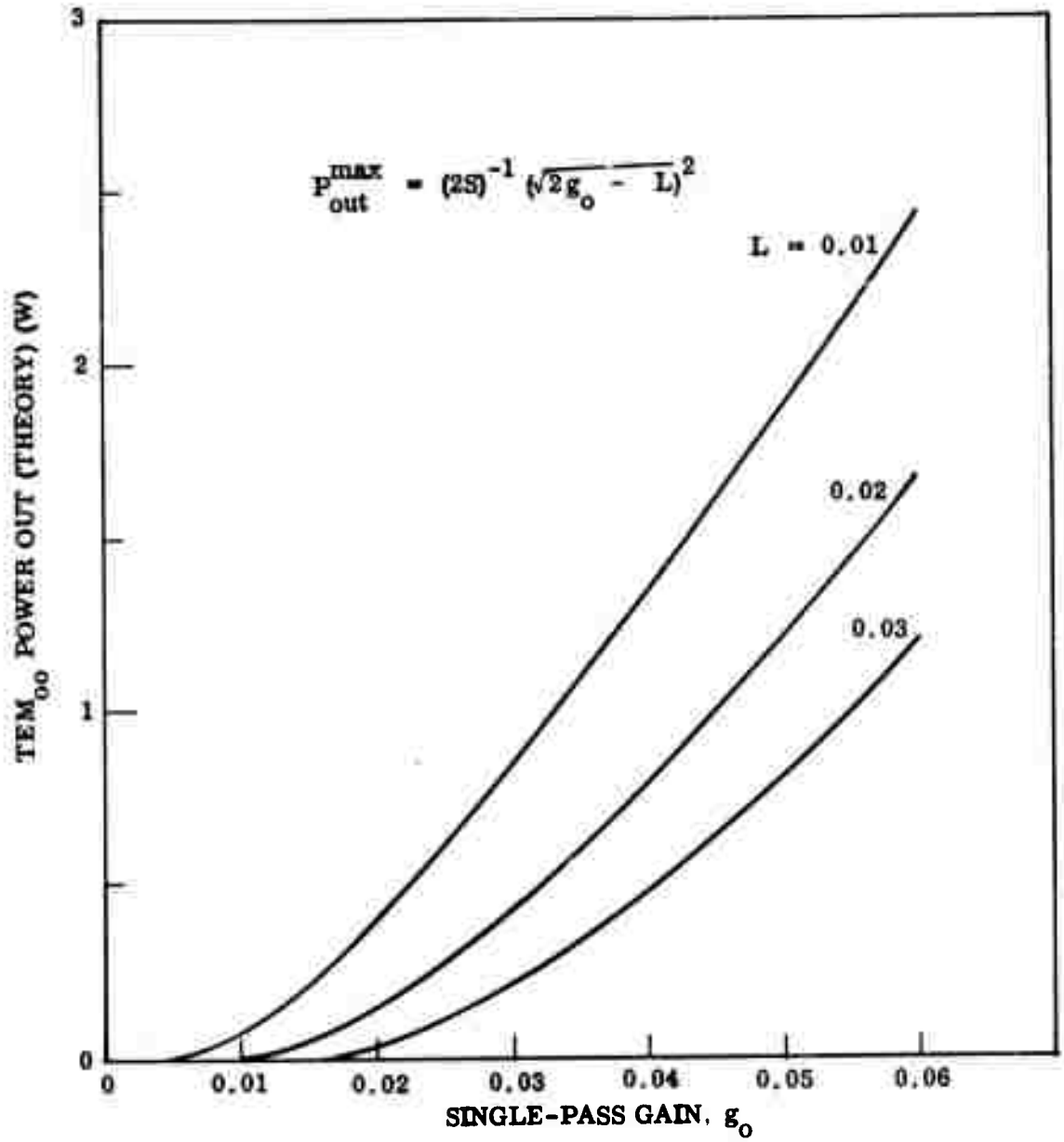

Fig. 2-6 Estimated TEM_{00} Laser Output Power for a Saturation Parameter $(2S)^{-1}$ = 40 W. The symbol L is the double-pass loss in the laser cavity. A waist radius of 1.2 mm in Nd:YAG is required for the saturation parameter assumed

2.1.3 Optimum Laser Rod Size

The optimum rod size is determined by the requirement of obtaining maximum gain and also maximum TEM_{oo} waist diameter in the rod in order to maximize the output power in accordance with Eqs. (2.3), (2.4), and (2.5). It is also influenced by the size of the lamp imaged onto the rod.

We have recently taken data on the intensity distribution across the diameter of a typical K-Rb lamp provided by ILC (Fig. 2-7). The lamp output was filtered at 8000 A to measure the useful spectral region. The full width at half-intensity is roughly 3 mm, although appreciable light is being emitted out to the full 5-mm bore diameter of the lamp. Thus for a rod having a diameter of only 3 mm, about 20% of the lamp radiation will miss the rod in a perfectly imaging cavity of unity magnification, while a 5-mm-diameter rod will intercept most of the lamp emission.

The useful rod diameter is more severely limited by the waist radius that can be achieved in a very stable TEM_{oo}-mode configuration. The waist radius can be made very large by approaching instability, such as is sometimes done by using plane resonator mirrors and a negative curvature on the laser rod to correct for thermal focusing. However, we have found such lasers to be extremely noisy.

We have devised and reported on cavity configurations for TEM_{oo}-mode operation that maximize the mode diameter in the rod while maintaining the stability of a near-confocal cavity (Refs. 2-9, 2-10). These configurations involve a flat mirror as one reflector, and a positive curvature surface on one end of the laser rod. The mode is focused to a very small waist near the other end mirror, which has a curvature of 5 to 10 cm. A stable waist radius of 1.2 mm in the rod can be achieved in a laser less than 50 cm long using this design. This waist is considerably larger than that achievable in the maximum stability region using designs without a focusing element.

To keep the aperture losses of the TEM_{oo}-mode to about 0.15% in one direction, the laser rod must have a radius that is about 1.8 times the waist radius. This rules

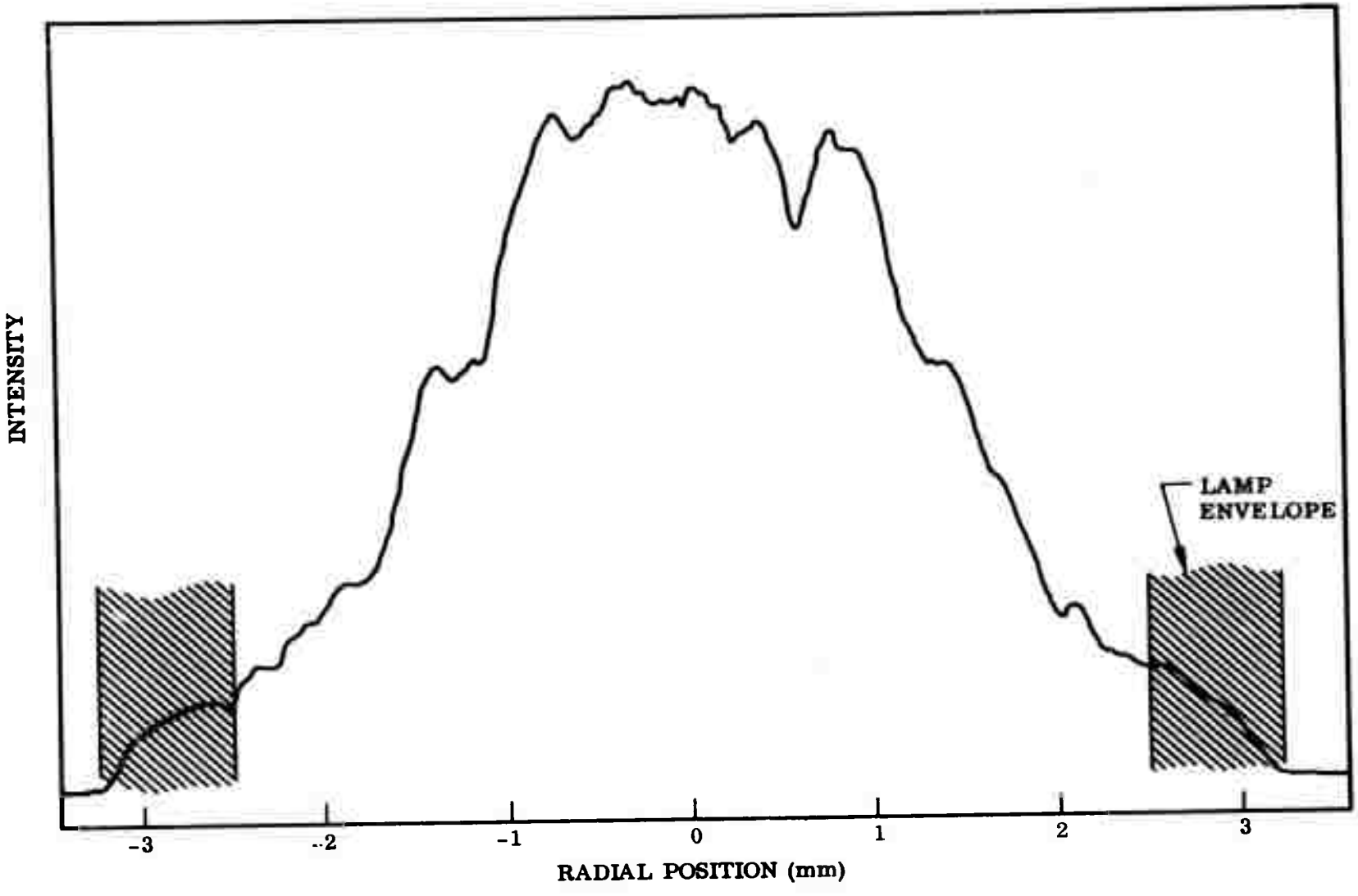

Fig. 2-7 Intensity Distribution Across the Image of a K-Rb Lamp

implies that the laser rod should have a clear diameter of about 4.3 mm for a 1.2-mm waist radius. This diameter is also about optimum for intercepting most of the useful lamp radiation. To account for beveling at the rod ends, the actual diameter may be increased to 5 mm.

The only factors that have an unknown influence are (1) the losses due to the thermal distortions, and (2) the optical attenuation of the pump radiation reaching the center of the rod. Initial consideration suggests that the distortion of a 5-mm rod should be no greater than in a somewhat smaller rod, and may be less because temperature gradients may be more uniform. The Nd:YAG rod at optimum Nd concentration is relatively thin optically for most of its pumping radiation, so only a small attenuation is expected in the extra 1-mm radius of the larger rod.

Selection of rod length is determined primarily by the maximum power loading permitted on the K-Rb lamps. At present, it appears that 50-mm-long lamps are necessary for handling 300 W with reasonable life expectancy, and the rod should be the same length. However, there is some advantage to using a shorter rod because of the initial -0.1%/cm negative gain due to thermal population of the terminal level. If lamp technology improves in the near future so that lamp loading can be increased, the option of choosing a rod length of less than 50 mm may be selected. A review of K-Rb lamp characteristics is given in Section 2.2.

2.2 POTASSIUM-RUBIDIUM (K-Rb) LAMPS

2.2.1 Background

The following material is a brief review of the K-Rb are lamps that are currently available from ILC, Inc. (Ref. 2-11). These alkali-vapor lamps are non-wall-stabilized lamps having spectra that closely match the excitation bands of Nd:YAG.

Because the alkali metals are solids at room temperature, the lamps are operated at elevated temperature. The envelope wall center temperature is maintained between

1000 and 1200°C, while the end caps are maintained at 600 to 800°C. Pressure and spectral regulation of the lamp is achieved by carefully controlling the alkali metal reservoir temperature.

The lamp structure consists of a sapphire envelope brazed to niobium end caps that are attached to tungsten metal electrodes and a tantalum reservoir. An outer vacuum quartz protective envelope protects the refractory metals and braze joint from oxidation. The lamps are radiation-cooled. Lamp construction techniques are illustrated in Fig. 2-8.

The lamps contains a low-pressure noble gas to aid starting. The lamps are ignited with a 10-kV pulse. A current-limited variable dc power supply with active or resistive ballast is employed to operate the lamps. Startup is accomplished by gradually increasing the dc power to the lamps over a period of several minutes.

The major resonance lines of the alkali metals used for pumping Nd:YAG are:

Potassium	7665 Å	7699 Å
Rubidium	7800 Å	7948 Å

The lamps normally operate at internal pressures of 50 to 200 Torr and have broadened and/or deeply reversed line spectra superimposed on a low-level continuum.

The lamp voltage is 35 to 80 V under steady-state operation. The lamps are designed for cw operation at an average wall loading between electrodes of 30 W/cm^2. Excursions to 100 W/cm^2 can be tolerated. Ninety-five percent of the input power of the lamps is transmitted as radiant energy. The lamp envelope itself reradiates a small amount of ir energy in the region of 1 to 5 μm. Approximately 38% of the input electrical energy is radiated in the 0.7- to 1.0-μ region. Lamps having 0.9-in. arc lengths operate at 55 to 65 V at the pressure required for optimum spectral matching to Nd:YAG.

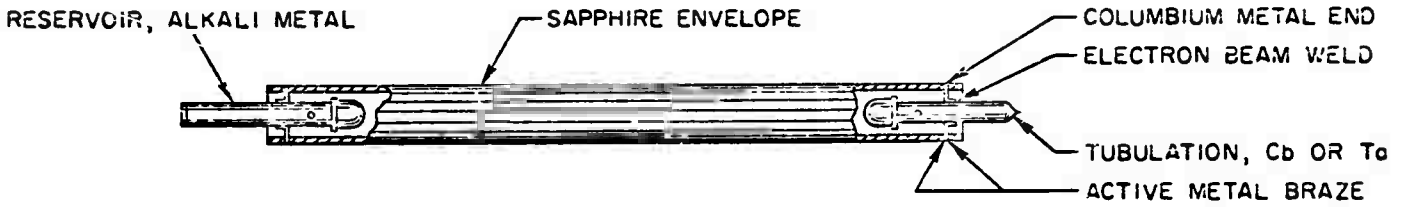

(a) BASIC ALKALI METAL LAMP - FOR USE IN VACUUM

(b) "NUDE" TUBE DESIGN - FOR USE IN AIR

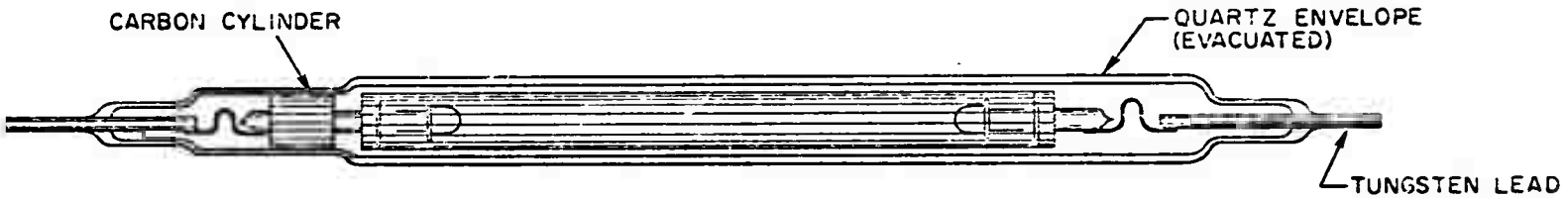

(c) QUARTZ ENVELOPE - FOR USE IN AIR OR LIQUID

Fig. 2-8 Alkali Vapor Lamps (Ref. 2-11)

A typical lamp spectrum between 0.5 and 1.7 μm, which is consistent with the infrared spectrum given in Section 2.1, is shown in Fig. 2-9. An excitation spectrum of Nd:YAG given in Fig. 2-10 supplements the absorption spectrum given in Section 2.1.

2.2.2 Evaluation of K-Rb Lamps

The lamps described in the preceding paragraphs have been used at LMSC for approximately a year. Experience gained using a close-coupled pumping cavity has indicated that heating of the K-Rb lamp, due to reflection of lamp radiation back onto the lamp in such a cavity, causes rapid deterioration of the lamp. Also, in a close-coupled pump cavity the laser rod is heated excessively, causing optical distortion and heat-removal problems.

The spectrum of the ir radiation from the lamp was shown in Section 2.1. The transmittance of an 8-mm-thick sample of sapphire at 1000°C is shown in Fig. 2-11 (Ref. 2-12). Since sapphire is black to radiation of wavelengths longer than 5 μm, that part of the lamp spectrum beyond 5 μm is due to radiation directly from the sapphire envelope. Approximately 20% of the power in the lamp spectrum is contained in the 4- to 10-μm spectral region. This radiation, if refocused on the lamp, will of course be reabsorbed in the sapphire.

Figure 2-12 (Ref. 2-13) shows spectra of K-Hg lamps operating at various pressures, with the spectrum at 240 Torr representing optimum coupling to the Nd:YAG absorption. As is expected, we observe strong line reversal due to the resonance transition at 0.7665 and 0.7699 μm. Some reversal is apparent for the lines near 1.15 and 1.25 μm, but the effect is much less than for the resonance transitions. We conclude that useful light refocused onto the lamp will be highly absorbed, at least near the center of the arc, whereas radiation between 1 and 1.5 μm will probably be reabsorbed only near the arc center and mostly transmitted through the rest of the arc. Therefore, the fraction of radiation absorbed in this spectral region when lamp light is refocused back onto the lamp should be small.

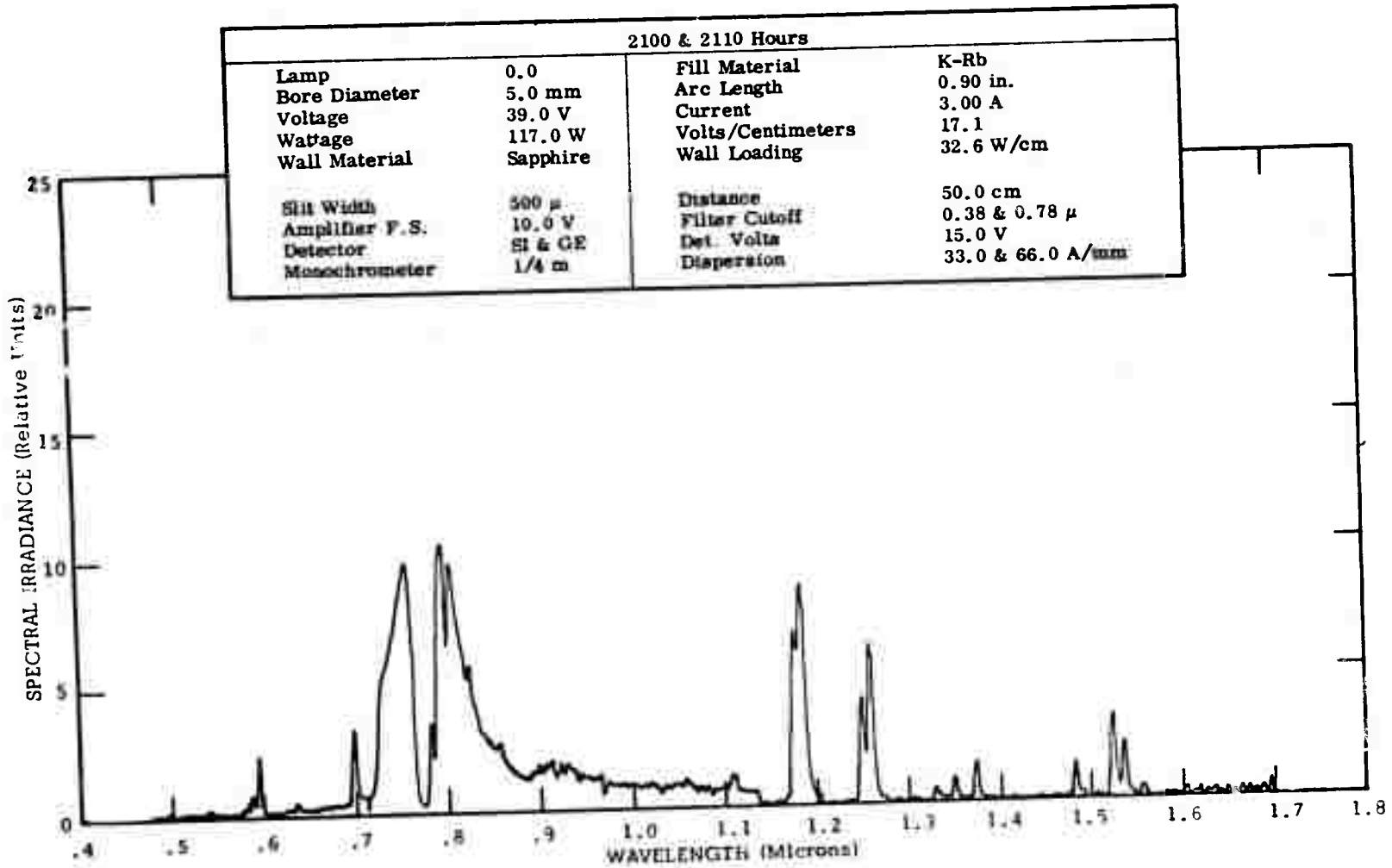

Fig. 2-9 Alkali Metal Lamp Spectrum (Ref. 2-11)

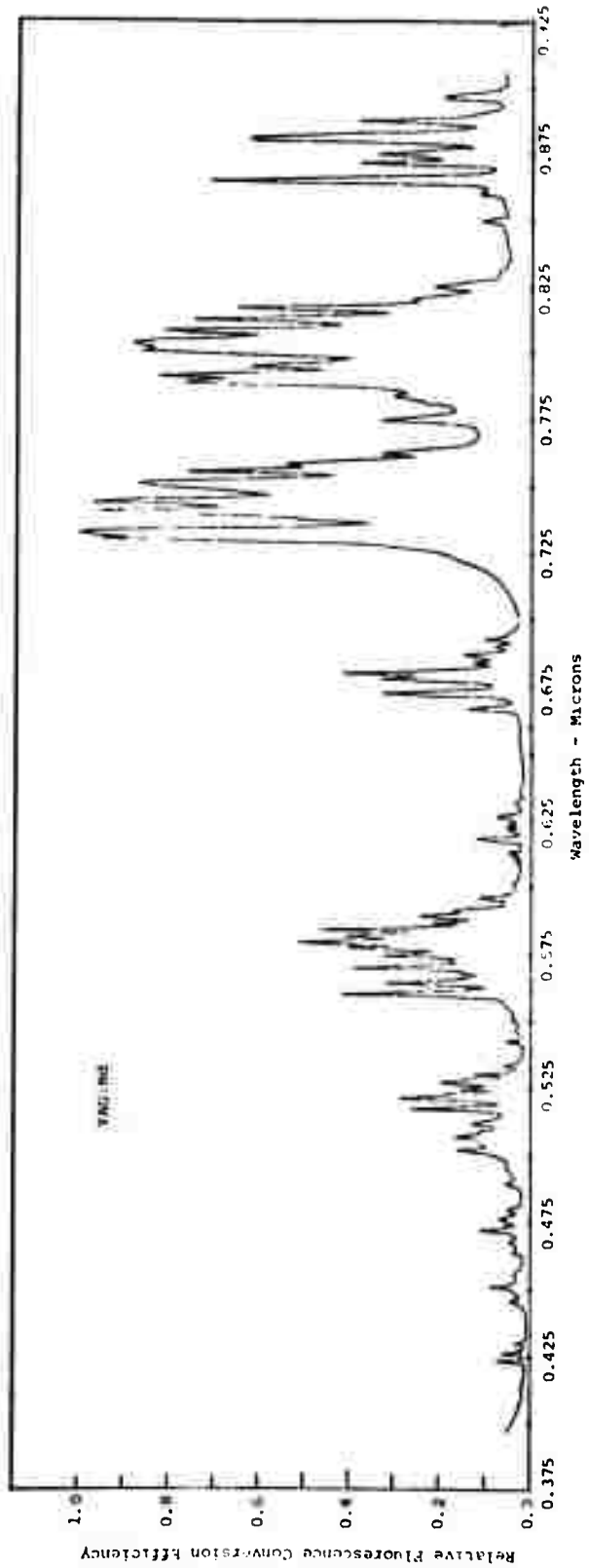

Fig. 2-10 Excitation Spectra for Nd:YAG (Ref. 2-11)

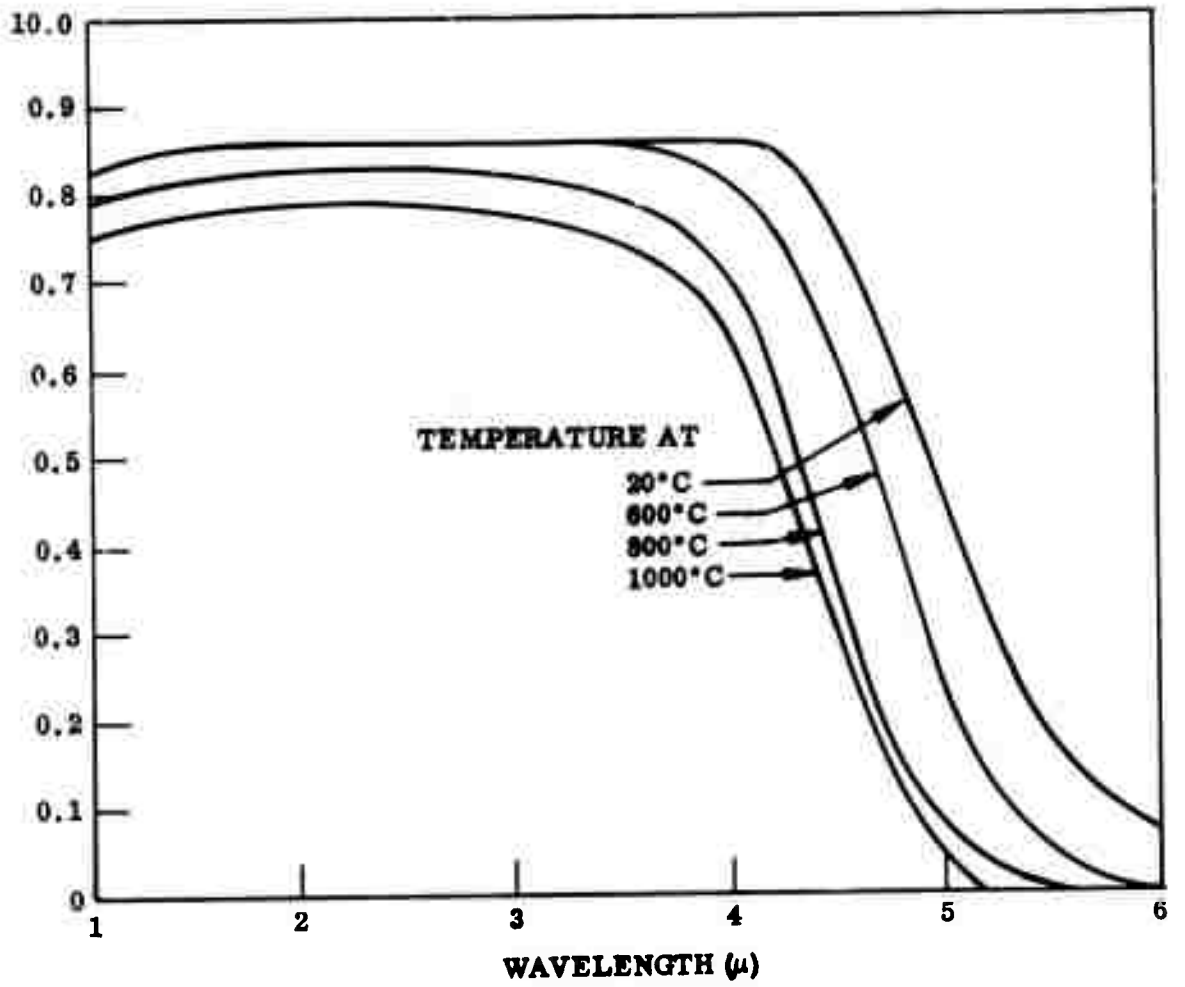

Fig. 2-11 Transmittance of Sapphire

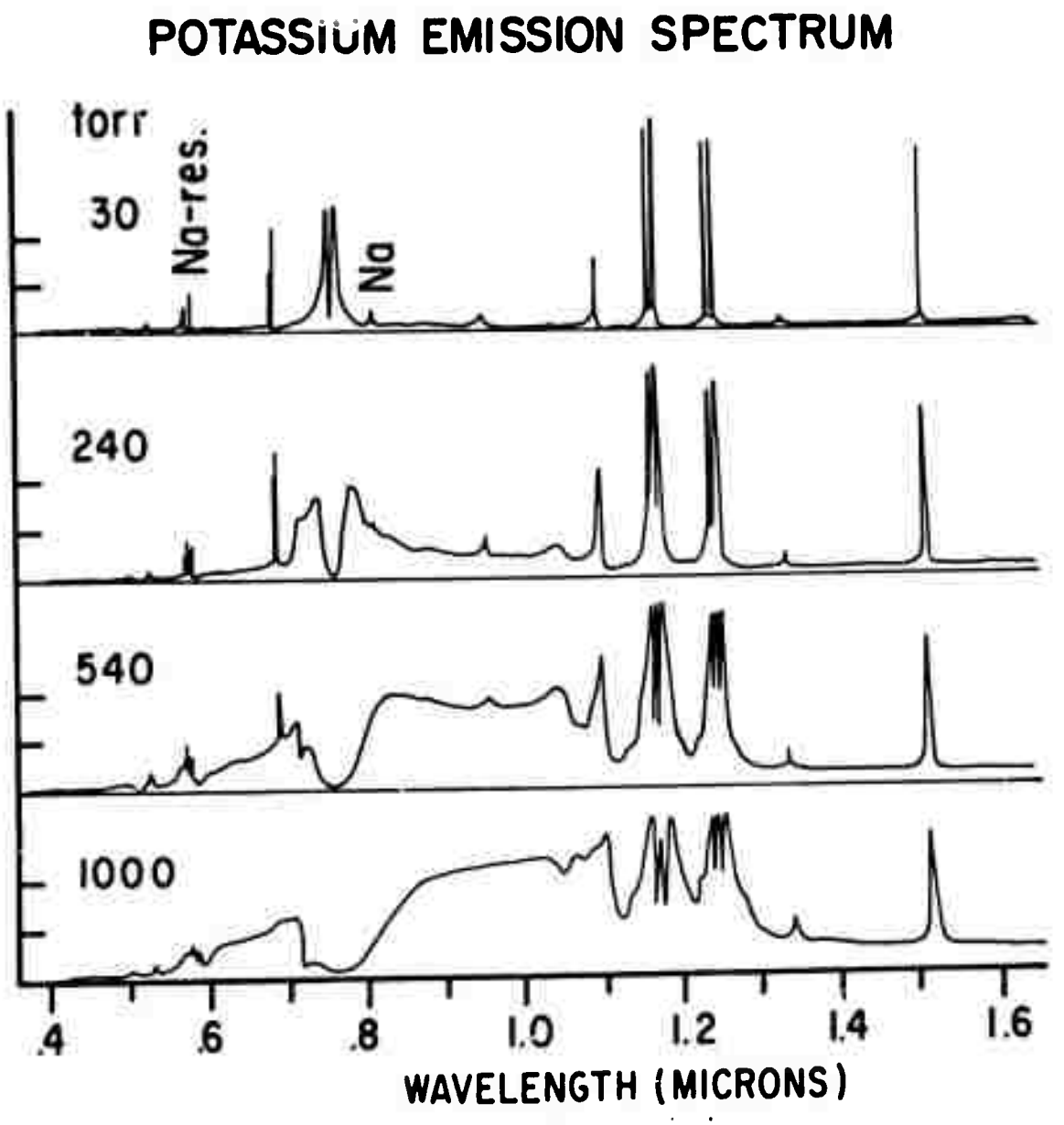

Fig. 2-12 Spectral Radiation From a Potassium Lamp (Ref. 2-13)

Absorption of wavelengths greater than 4 μm in the sapphire envelope and the resultant rise in wall temperature are presumed to constitute the major factor in the reduction of lamp life. Resonance radiation that is absorbed should be reradiated as useful light. The degree to which absorption of the 1- to 1.5-μm radiation will affect efficiency or lamp life is not clear. Our primary concern, then, for protection of the lamp, is preventing emitted radiation of wavelengths longer than 4 μm from returning to the lamp.

For purposes of cavity design and estimation of pumping efficiency, the profile of the arc has been measured for a quartz-jacketed lamp operating at optimum pressure for a Nd:YAG laser. The profile was measured by focusing the image of the lamp onto the slit of a scanning device incorporating an S1 photomultiplier. Profiles were measured with and without a filter to pass only radiation of wavelengths of 0.7 to 0.9 μm. A typical scan was shown in Fig. 2-7. Since the S1 photocathode is sensitive primarily to useful light, no difference in the profile was observed using the filter.

2.3 PLANS FOR NEXT QUARTER

The emphasis in this report has been on the background information measured and collected on this program which is necessary to significantly increase the efficiency of the Nd:YAG laser. Single-frequency mode filter studies also continued producing higher-power outputs with increased laser stability. These results will be reported in detail in the Semi-Annual Report.

Work is progressing on building a more stable laser cavity configuration, with optimized adjustment mechanisms which we have found so essential for both maximum stability and power output.

New spherical pump cavity designs have been ordered, based on a thermal analysis using K-Rb lamps. These lamps will significantly decrease the waste heat that must be removed by the water filter, and therefore will improve stability.

Further experiments with several different-diameter K-Rb lamps are underway to determine the optimum lamp and rod diameters for maximum efficiency. Measurements of gain profiles across the laser rod will assist in this determination.

2.4 REFERENCES

2-1 T. Kushida, "Linewidths and Thermal Shifts of Spectral Lines in Nd:YAG and Calcium Fluorophosphate," Phys. Rev., Vol. 185, 1969, pp. 500–508

2-2 L. Noble et al., Optical Pumps for Lasers, ECOM-0035-F, Final Report on Contract DAAB07-70-C-0035, ILC, Inc., May 1971, p. 100

2-3 I. Liberman, D. A. Larson, and C. H. Church, "Efficient Nd:YAG Lasers Using Alkali Additive Lamps," IEEE J. Quant. Elect., Vol. QE-5, May 1969, p. 238

2-4 J. E. Geusic et al., "Continuous 0.532 μm Solid-State Source Using $Ba_2NaNb_3O_{15}$," Appl. Phys. Lett., Vol. 12, May 1968, pp. 306–308

2-5 R. Polloni and O. Svelto, "Static and Dynamic Behavior of a Single-Mode Nd:YAG Laser," IEEE J. Quant. Elect., Vol. QE-4, Aug 1968, pp. 481–484

2-6 T. Kushida, H. Marcos, and J. E. Geusic, "Laser Transition Cross Section and Fluorescence Branching Ratio for Nd^{3+} in YAG," Phys. Rev., Vol. 167, Mar 1968, pp. 289–291

2-7 J. D. Foster and R. F. Kirk, Space Qualified Nd:YAG Laser, Final Technical Report on Contract NAS12-2160, Jun 1970

2-8 I. Liberman et al., Optical Pumps for Lasers. Phase II, ECOM-02097-F, Final Report on Contract DA-28-043-AMC-02097(E), Oct 1968, Figs. 145 and 146

2-9 R. C. Ohlmann, "Component Characteristics for a Wideband FM/IM Optical Data Relay System," Proc. of 4th Conf. on Laser Technology, Jan 1970, pp. 1401–1409

2-10 R. C. Ohlmann et al., High-Efficiency, Single-Frequency Laser and Modulator Study, 3rd Quarterly Summary Technical Status Report, Contract N00014-71-C-0049, Jul 1971

2-11 "Alkali Vapor Lamps for Lower Power Nd:YAG Lasers," Engineering Note 10, ILC, Inc., Sunnyvale, Calif.

2-12 U. P. Oppenheim and U. Even, J. Opt. Soc. Am., Vol. 52, 1962, p. 1078

2-13 K. Schmidt, Proc. 6th Int. Conf. on Ionization Phenomena in Gases, Vol. 3, Paris, 1963, pp. 323–330

Section 3

WIDE-BANDWIDTH ELECTROOPTICAL MODULATOR

3.1 DESIGN OF 2- TO 4-GHz ELECTROOPTICAL MODULATOR

During this quarter, the design and fabrication of the first-model 2- to 4-GHz electro-optical modulator were completed. In order to accommodate the capacitance of $LiNbO_3$ crystals 5 to 7 mm long in the output gap, the digits had to be considerably foreshortened compared to those in the 1- to 2-GHz modulator. In fact, it was found that for an output capacitance of 1.33 pF, corresponding to that of a $LiNbO_3$ crystal of square cross section and 5-mm length, and using the published value of the low-frequency dielectric constant, the maximum allowable electrical length of the digit was only 30 deg for 50-Ω input and output impedances. To minimize complications and uncertainties in the first model, conventional design methods using four 30-deg digits at 50-Ω input and output impedance levels were used. However, this demanded a substantially different modulator configuration from the conventional bandpass filter design.

The following design parameters were obtained using computer analysis:

- Center frequency: 3 GHz
- Bandwidth: 83.7%
- Attenuation ripple: 0.01 dB
- Number of digits: 4
- Digit length: 30 deg at center frequency
- Input impedance: 50 Ω
- Output impedance: 50 Ω

The resultant dimensions calculated are as shown in Fig. 3-1.

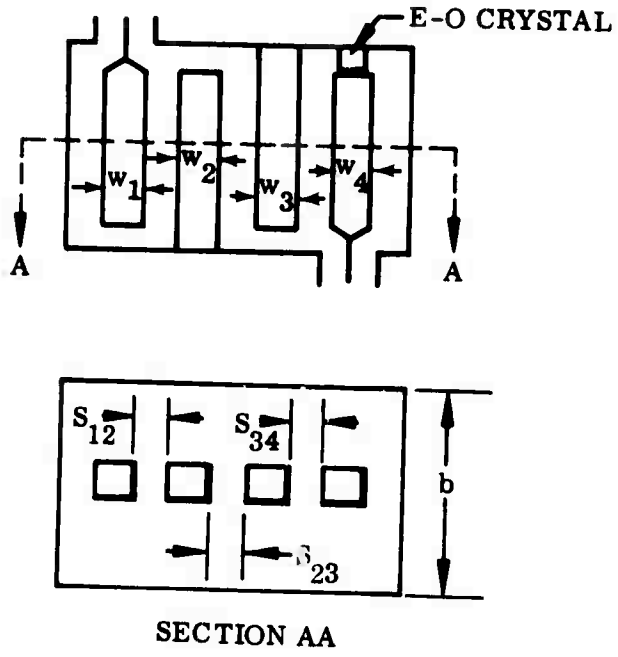

$w_1 = 0.049$
$w_2 = 0.049$
$w_3 = 0.049$
$w_4 = 0.049$

$S_{12} = 0.014$
$S_{23} = 0.043$
$S_{34} = 0.014$

$t = 0.030$
$b = 0.400$

Values in inches

Fig. 3-1 The 2- to 4-GHz Modulator Design, Input and Output Impedances of 50 Ω

This design gave the allowable capacitance at the output gap of 1.33 pF, which, as mentioned earlier, corresponded to that of a $LiNbO_3$ crystal of 5-mm length, neglecting stray capacitances. However, past experience in the 1- to 2-GHz region had indicated that the actual microwave capacitance of $LiNbO_3$ was somewhat less than the published low-frequency values. Hence, it was felt that, with this design, crystals up to 7 mm in length could be accommodated.

This design was chosen and a modulator was fabricated. An x-ray photograph of the modulator is shown in Fig. 3-2 in which the significant parts are labeled. This figure shows that, because of the smallness of the dimensions, some compromise has to be made in the realization of the design, especially in the input-output connections. It is also seen from this figure that a dc blocking capacitor has been included in the ground side of the output digit to allow electrooptic compensation to be used during modulator tests.

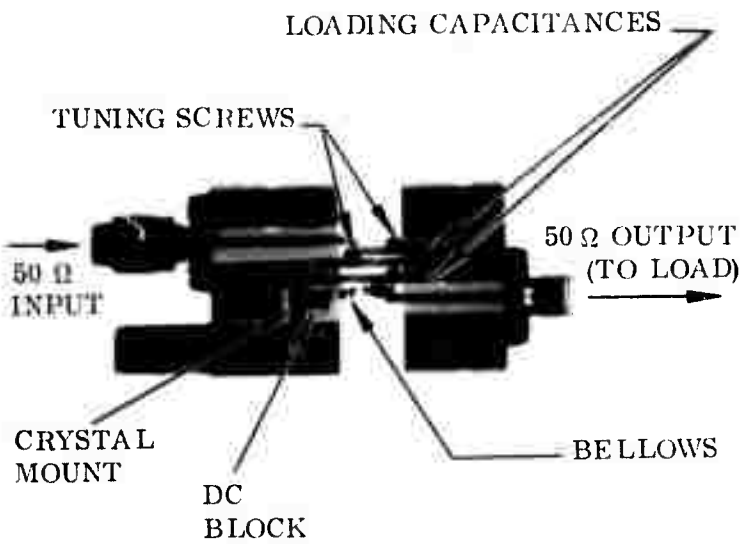

Fig. 3-2 X-Ray Photograph of the First Model 2- to 4-GHz Modulator, Showing Details of Construction

3.2 RF TESTS

After fabrication, the modulator was tuned for the best rf response in the 2- to 4-GHz band using $LiNbO_3$ crystals of different dimensions and consequently of different capacitances. This was done to ensure that the longest crystal, which would give the best modulation index, could be matched to the circuit without sacrificing bandwidth. Some of the test results of VSWR and insertion loss as a function of frequency are shown in Figs. 3-3A, B, and C for crystals of lengths 5.6, 7.0 and 7.5 mm, respectively. Although the 5.6-mm crystal (Fig. 3-3A) gave the best VSWR, both the 7.0- and 7.5-mm crystals gave good results. The 7.5-mm crystal did not have gold electrodes on its C-faces; therefore, the effective capacitance in the gap could be somewhat lower than the actual capacitance because of nonuniform contact. This lower effective capicitance gave rise to an apparently good rf match. On the other hand, the insertion losses for the 7.0- and 7.5-mm crystals were substantially the same, in spite of the

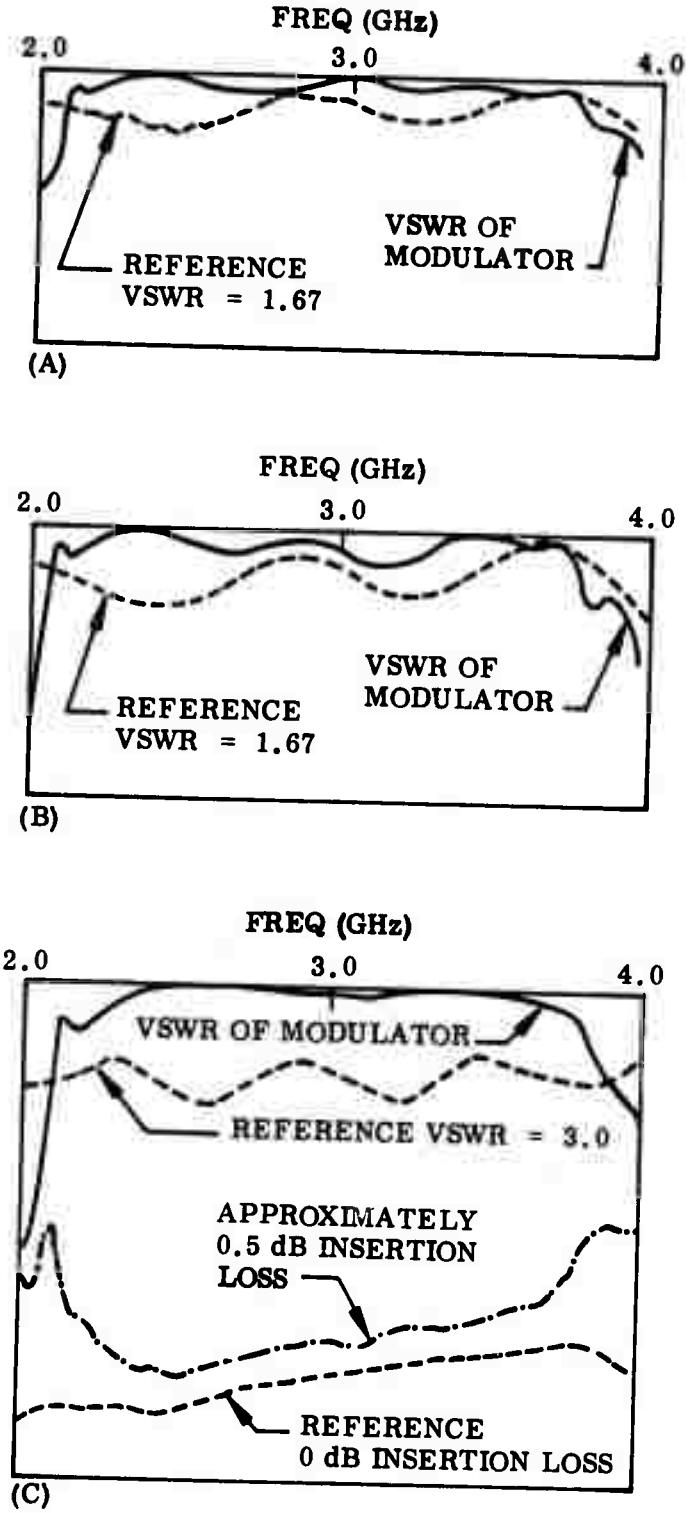

Fig. 3-3 RF Test Results of the Modulator Using Different $LiNbO_3$ Crystals: (A) 5.6-mm length with gold electrodes; (B) 7.0-mm length with gold electrodes; and (C) 7.6-mm length without electrodes. The cross sections of these crystals are approximately square

absence of gold electrodes on the longer crystal. From these results, it was concluded that this circuit could accommodate an $LiNbO_3$ crystal of at least 7 mm in length.

During the rf testing, it was found that spurious resonances at 2.16 and 3.8 GHz were present; these resonances were not affected to any degree by tuning. They were detected in the VSWR and insertion loss curves, and are most evident in the latter (Fig. 3-3C). The presence of these spurious resonances resulted in high absorptions at the aforementioned frequencies; hence, for a given tuning, the VSWR and insertion loss curves looking into the input were quite different from those looking into the output. However, over the major portion of the 2- to 4-GHz band (2.2 to 3.7 GHz), the VSWR and insertion loss were small and flat looking into either port. Shorting out the dc blocking capacitor eliminated these spurious resonances.

This experience agreed well with that obtained in the tuning of the 19-Ω 1- to 2-GHz modulator (Model 2) in the fourth quarter. It will be recalled that, in that case, two blocking capacitors were employed, resulting in one spurious resonance at about 1.2 GHz. In the present case, only one capacitor was used, giving rise to the two resonances just described. All such resonances disappeared when the capacitors were shorted out. It is clear, therefore, that these resonances are associated with the blocking capacitors. To eliminate them, the crystal mount must be carefully redesigned either by using different blocking schemes or by incorporating some for of rf choke. This redesign is in progress. Meanwhile, the modulator in its present form will be tested for modulation performance during the next quarter to ascertain its useful range.

3.3 DETECTION TECHNIQUES IN THE 2- to 4-GHz BAND

At present, no photodetector has a flat response (if any response at all) much above 2 GHz. To determine the modulation index of the 2- to 4-GHz modulator, either indirect measurements or photodetectors having a calibrated frequency response must be used. Three such techniques relating to the 1- to 2-GHz band have been

presented elsewhere (Ref. 3-1), so only extension to the 2- to 4-GHz band will be discussed here. The three techniques are:

- Phase-Retardation Measurement. In this method, the optical bias is adjusted to give either maximum or minimum light transmission through the modulator in the absence of a modulating signal. When the modulation power is applied, phase retardation between the ordinary and the extraordinary rays occurs, resulting in an average change of light transmitted. This change in intensity gives a measure of the retardation angle, from which the modulation index may be calculated. Since this method measures only the average change over many microwave cycles, it is as applicable to the 2- to 4-GHz band as to the 1- to 2-GHz band.
- Sideband Power Measurement. In this measurement, the optical sideband power due to modulation P_+ and the optical carrier power P_c are measured at various optical biases using an optical scanning interferometer. It has been shown (Ref. 3-1) that, for $LiNbO_3$, the modulation index M_d is given by

$$M_d = 2J_1 (2.08 \sqrt{P_+/P_c}) \quad \text{at } 0° \text{ or } 180° \text{ optical bias, or} \tag{3.1}$$

$$M_d = 2J_1 (1.852 \sqrt{P_+/P_c}) \quad \text{at } 90° \text{ optical bias} \tag{3.2}$$

The relative phase retardation angle $\Delta\Gamma$ between the ordinary and extraordinary rays is given by

$$\Delta\Gamma = 2.80 \sqrt{P_+/P_c} \quad \text{at } 180° \text{ bias, or} \tag{3.3}$$

$$\Delta\Gamma = 1.852 \sqrt{P_+/P_c} \quad \text{at } 90° \text{ bias} \tag{3.4}$$

Again, since the measurement is essentially concerned with a dc measurement of optical power transmitted through a tuned Fabry-Perot interferometer, it will not depend on the modulation frequency. This method does require a stable, single-frequency laser as the optical carrier.

- Substitution Measurement Using a Calibrated Photodetector. This method, in which a known rf signal is used to match the rf output of a photodetector, is the simplest of all in concept. However, to obtain a calibration for the photodiode for use in the 2- to 4-GHz band is not a simple matter. For calibration in the 1- to 2-GHz region, first-order Bragg-diffracted waves from an ultrasonic/optical interaction were mixed in a photodiode to give a 100% modulated signal (at a frequency twice that of the ultrasonic wave). Unfortunately, this technique cannot be extended to the 2- to 4-GHz band because of equipment limitations.

One method of calibrating the detector is to use an electrooptical modulator having a reasonably flat frequency response in the 1- to 2-GHz band and optically biased at maximum transmission. Under such conditions, only the second and other even harmonics of the modulation signal will be detected, as can be clearly seen from Fig. 3-4.

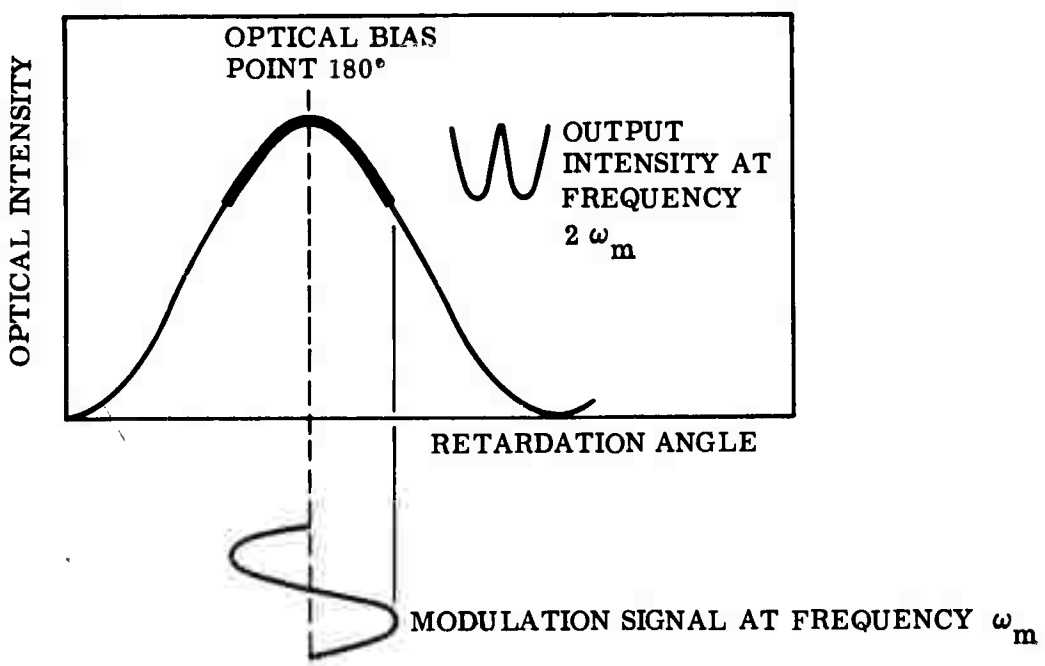

Fig. 3-4 Modulated Output Intensity at 180-deg Bias

The output intensity $I(\omega_m t)$ at 180 deg (or π radian) optical bias, after passing through a crossed analyzer, may be written as

$$I(\omega_m t) = \frac{1}{2}\left(\frac{E_o}{2}\right)^2 \left\{2 - \exp\left[- j\pi + j\theta_o (\Delta n_e - \Delta n_o) \sin \omega_m t\right] - \exp\left[+ j\pi - j\theta_o (\Delta n_e - \Delta n_o) \sin \omega_m t\right]\right\} \tag{3.5}$$

where

E_o = amplitude of the optical electric vector at the input to the modulator

θ_o = optical phase angle in free space corresponding to the crystal length ℓ, [i.e., $\theta_o = (\omega_o/c)\,\ell$]

Δn_e and Δn_o = changes of refractive indexes for extraordinary and ordinary rays due to the modulation voltage E_{zm}

That is,

$$\Delta n_e - \Delta n_o = \frac{1}{2}\left(n_o^3 r_{13} - n_e^3 r_{33}\right) E_{zm} \tag{3.6}$$

where the n's and the r's have their usual meanings.

Therefore, the relative phase retardation angle $\Delta\Gamma$ is given by

$$\Delta\Gamma = \theta_o (\Delta n_o - \Delta n_e) \tag{3.7}$$

Rewriting Eq. (3.5), we find

$$I(\omega_m t) = \frac{E_o^2}{8}\left\{2 + \exp[-j\Delta\Gamma \sin \omega_m t] + \exp[j\Delta\Gamma \sin \omega_m t]\right\}$$

$$= \frac{E_o^2}{4}[1 + \cos(\Delta\Gamma \sin \omega_m t)]$$

$$= \frac{E_o^2}{4}\left\{1 + J_o(\Delta\Gamma) + 2[J_2(\Delta\Gamma)\cos 2\omega_m t + J_4(\Delta\Gamma)\cos 4\omega_m t + \cdots]\right\} \tag{3.8}$$

Therefore, the modulation index at $2\omega_m$, M_2, is given by

$$M_2 = 2J_2(\Delta\Gamma) \tag{3.9}$$

$$\approx \left(\frac{\Delta\Gamma}{2}\right)^2 \quad \text{for} \quad \Delta\Gamma \leq 0.5 \tag{3.9A}$$

If, at the same time that M_2 is being measured, the sideband measurement is also made, then $\Delta\Gamma$ will be given by Eq. (3.3). On the other hand, because of the rolloff of the photodetector response with frequency, the apparent modulation index at $2\omega_m$, M_2' will be less than M_2. Therefore, by measuring both quantities, a calibration curve for the detector may be obtained.

It may appear that this method is worse than the sideband measurement method because additional uncertainties – the photodetector response and match – are introduced. However, because the sideband method does require a stable single-frequency laser as the optical carrier, as well as proper mode matching into the scanning interferometer, a calibrated detector does offer convenience and versatility in laboratory use. Of course, it is of paramount importance that all due care be taken to eliminate errors during calibration.

With proper care in the processes of measurement and calibration, the results obtained by the above three methods should agree within a few percent.

3.4 CRYSTAL FABRICATION

Continuing effort on crystal fabrication under LMSC's in-house program is being carried out during this quarter. Extinction ratios of 25 dB have been obtained for select 0.3 × 0.25 × 5-mm 0.3 × 0.25 × 7-mm $LiNbO_3$ crystals.

3.5 FUTURE PLANS

For the next quarter, tests on modulation depths of the 2- to 4-GHz modulator already fabricated will be made. The bandwidth limitations due to the spurious resonances will be ascertained. The dc-block/rf-ground in the crystal mount will then be modified to obtain the designed bandwidth. Detector calibration will be carried out. The three detection methods discussed above will be used for the modulation measurements. Some of the crystals fabricated at LMSC which have good extinction ratios will be sent out to have gold electrodes and AR coatings deposited on the various proper faces.

3.6 REFERENCES

3-1 K. K. Chow and W. B. Leonard, "Efficient Octave-Bandwidth Microwave Light Modulators," IEEE J.Q.E., Vol. QE-6, Dec 1970, pp. 789–793